


RESEARCH PAPER

Thrombin modifies growth, proliferation and apoptosis of human colon organoids: a protease-activated receptor 1- and protease-activated receptor 4-dependent mechanism

Correspondence Dr Nathalie Vergnolle, Inserm UMR-1220, Institut de Recherche en Santé Digestive, CS60039 CHU Purpan, 31024 Toulouse, Cedex-3, France. E-mail: nathalie.vergnolle@inserm.fr

Received 20 December 2017; **Revised** 24 April 2018; **Accepted** 8 June 2018

Morgane Sébert¹, Alexandre Denadai-Souza¹, Muriel Quaranta¹, Claire Racaud-Sultan¹, Sophie Chabot², Philippe Lluel², Nicolas Monjot³, Laurent Alric⁴, Guillaume Portier⁵, Sylvain Kirzin⁵, Delphine Bonnet¹, Audrey Ferrand^{1,*} and Nathalie Vergnolle^{1,5,*} 

¹IRSD, Université de Toulouse, INSERM, INRA, ENVT, UPS, Toulouse, France, ²UROsphere, Ramonville, France, ³Institut de Recherche Pierre Fabre, Castres, France, ⁴Department of Internal Medicine and Digestive Diseases, CHU Purpan, Toulouse, France, and ⁵Department of Physiology and Pharmacology, University of Calgary, Calgary, AB, Canada

*Audrey Ferrand and Nathalie Vergnolle are joint last authors.

BACKGROUND AND PURPOSE

Thrombin is massively released upon tissue damage associated with bleeding or chronic inflammation. The effects of this thrombin on tissue regrowth and repair has been scarcely addressed and only in cancer cell lines. Hence, the purpose of the present study was to determine thrombin's pharmacological effects on human intestinal epithelium growth, proliferation and apoptosis, using three-dimensional cultures of human colon organoids.

EXPERIMENTAL APPROACH

Crypts were isolated from human colonic resections and cultured for 6 days, forming human colon organoids. Cultured organoids were exposed to 10 and 50 mU·mL⁻¹ of thrombin, in the presence or not of protease-activated receptor (PAR) antagonists. Organoid morphology, metabolism, proliferation and apoptosis were followed.

KEY RESULTS

Thrombin favoured organoid maturation leading to a decreased number of immature cystic structures and a concomitant increased number of larger structures releasing cell debris and apoptotic cells. The size of budding structures, metabolic activity and proliferation were significantly reduced in organoid cultures exposed to thrombin, while apoptosis was dramatically increased. Both PAR1 and PAR4 antagonists inhibited apoptosis regardless of thrombin doses. Thrombin-induced inhibition of proliferation and metabolic activity were reversed by PAR4 antagonist for thrombin's lowest dose and by PAR1 antagonist for thrombin's highest dose.

CONCLUSIONS AND IMPLICATIONS

Overall, our data suggest that the presence of thrombin in the vicinity of human colon epithelial cells favours their maturation at the expense of their regenerative capacities. Our data point to thrombin and its two receptors PAR1 and PAR4 as potential molecular targets for epithelial repair therapies.

Abbreviations

IBD, inflammatory bowel disease; NAC, N-acetylcysteine; PAR, protease-activated receptor; PFA, paraformaldehyde; RT, room temperature

Introduction

A new paradigm has been set up for the treatment of inflammatory bowel diseases (IBDs), shifting from resolving symptoms and inflammation *per se* (i.e. infiltration and activation of inflammatory cells), towards the objective of tissue repair and mucosal healing (Iacucci and Ghosh, 2016). Indeed, mucosal healing and epithelial repair are increasingly incorporated in the outcome measures of clinical trials (Shah *et al.*, 2016). This new focus on epithelial regeneration and healing has shed new light on intestinal epithelial cell biology and drives a new area of research for the development of therapeutic approaches for IBD. The study of mediators that are released in the course of chronic intestinal inflammation and their effects on epithelial biology has become a major focus of research for drug development.

In that setting, **thrombin** appears as a most important candidate, since IBD patients exhibit abnormalities in coagulation and fibrinolysis, have an increased thrombin generation and a significant presence of this protease in colonic tissues (de Jong *et al.*, 1989; Senchenkova *et al.*, 2015). Therefore, the effects of thrombin on human epithelial tissues have to be carefully considered. Previous studies have investigated the effects of thrombin on intestinal cancer cell lines (Darmoul *et al.*, 2003), demonstrating that thrombin provoked dramatic mitogenic responses, proliferation and increased cell migration. These studies suggested that thrombin could be a growth factor for human colon cancer. However, the effects of thrombin on intestinal epithelium have only been studied in cancer cells, which are known to overexpress thrombin receptors (Darmoul *et al.*, 2003; Gratio *et al.*, 2009). What are the effects of thrombin chronic exposure on non-transformed and non-cancerous human intestinal epithelial cells? Does thrombin modify epithelial proliferation, apoptosis of non-cancerous cells or regeneration in intestinal tissues? Does the presence of thrombin modify epithelial repair in the context of IBD?

The recent development of human colon organoid cultures allows pharmacological testing of compounds in three-dimensional (3D) primary cell cultures in complex human epithelia (Sato *et al.*, 2011; Crespo *et al.*, 2017). Indeed, organoid cultures are representative of the complex composition of intestinal epithelium, since within the same organoid, after a few days of culture, stem cells, progenitors and differentiated cells are detected (Sato *et al.*, 2011). In the present study, we took advantage of this model to test the effects of thrombin on human healthy epithelium. This model replicates the cell composition of a physiological epithelium, and, therefore, pharmacological approaches using a more physiological model are also more relevant to predict a drug's effects. Since renewal of damaged epithelium and epithelial repair implicate cell survival, growth and proliferation, our aim was to determine the effects thrombin has on these parameters in human colon organoid cultures and to study the potential involvement of the two active thrombin receptors: protease-activated receptor (**PAR**)1 and **PAR**4.

Methods

Human samples

Biological samples were obtained from five different patients treated at the Toulouse University Hospital. Patients gave informed consent and were included in the registered COLIC study (DC-2015-2443). Colonic samples were obtained from surgical resections of patients suffering from colorectal cancer. Tissues that were used were harvested in healthy zones at the margin of the resection and at least 10 cm away from the tumour. Characteristics and treatments of patients are provided in Supporting Information Table S1.

Organoid cultures

Tissue obtained was opened longitudinally and washed with Dulbecco's PBS (DPBS; Sigma-Aldrich #D8537, Saint-Quentin-Fallavier, France). Then, the mucosa was removed and incubated in an antibiotic solution (gentamicin Sigma-Aldrich #G1397, Saint-Quentin-Fallavier, France, 1000×; normocin InvivoGen #ANT-NR-1, Toulouse, France, 500×; and fungizone Gibco #15290-018, Illkirch, France, 100×) for 5 min at room temperature (RT), four times. The mucosa was cut into 0.2- to 0.5-cm-long pieces and placed in a Petri dish containing cold DPBS before a series of three incubations in a 10 mM DTT (Roche #10197777001, Meylan, France) solution, for 5 min at RT. Pieces of tissue were transferred into a 8 mM EDTA (Ambion #L/N.1408029, Dardilly, France) solution and were left under gentle rocking for 1 h at 4°C. Supernatants were removed and replaced by 10 mL of DPBS. Mucosa fragments were then resuspended by vigorous manual up and down shaking (at least 15 repeated movements). Supernatants were recovered into a new 15 mL falcon tube and centrifuged for 2 min, 40× g at 4°C. Ten millilitres of DMEM/F12 (Invitrogen #12634-010, Illkirch, France) supplemented with 100× Glutamax-CTS (Invitrogen #A1286001, Illkirch, France), 100× HEPES (Gibco #15630-056, Illkirch, France) and 5% FBS was added to the pellets and centrifuged again for 2 min, 40× g at 4°C. This step was repeated twice. Then, crypts were counted in a 20 µL drop and the samples were centrifuged once again for 2 min, at 40× g at 4°C. Supernatants were removed, and fresh hES Matrigel (Corning #354277, Amsterdam, Netherlands) was added to the pellets, carefully avoiding air bubbles. Ten microlitres of Matrigel containing 20 crypts were plated in each well of a pre-warmed 96-well plate (Ibidi, Martinsried, Germany µ-angiogenesis). Once the Matrigel had polymerized for 20 min, 70 µL of culture medium was added to each well. The culture medium was composed of 50% advanced DMEM/F12, 50% **Wnt3a**-conditioned medium [supernatants from L Wnt-3A cells (ATCC® CRL-2647™)], 100× Glutamax-CTS, 100× HEPES, serum-free B27 (Life Technologies #12587-010, Villebon-sur-Yvette, France, 50×), N2 (Invitrogen #17502-048, Illkirch, France 100×), *N*-acetylcysteine (NAC; Sigma #A9165-5G, Saint-Quentin-Fallavier, France 500×), nicotinamide (Sigma #N0636, Saint-Quentin-Fallavier, France 10 mM), recombinant human epithelial growth factor (Gibco #PHG0314, Illkirch, France 50 ng·mL⁻¹), human Noggin (Tebu #120-10C, Le-Perray-en-Yvelines, France 100 ng·mL⁻¹), human R-spondin (R&D #4645RS, Lille, France 1 µg·mL⁻¹), gastrin (Sigma G9145, Saint-Quentin-Fallavier, France 10 nM),

SB202190 (Sigma 57067, Saint-Quentin-Fallavier, France 10 μM), **LY2157299** (Axon MedChem #1941, Groningen, Netherlands 0.5 μM) and **PGE₂** (Sigma #P0409, Saint-Quentin-Fallavier, France 0.01 μM). The cultures were finally incubated in a humidified incubator at 37°C and 5% CO₂. The culture medium was changed every 3 days but without NAC and LY2157599.

Treatments with thrombin and antagonists

Thrombin (Sigma-Aldrich #T6884, Saint-Quentin-Fallavier, France) diluted in 0.1% BSA (Sigma-Aldrich #A9576, Saint-Quentin-Fallavier, France) was added to culture media daily starting from day 3 and until day 6, at two different doses: 10 and 50 $\text{mU}\cdot\text{mL}^{-1}$. Forty-five minutes before each addition of thrombin to culture media, the PAR1 antagonist **F16357** (Pierre Fabre Medicaments, Toulouse, France), PAR4 antagonist **ML354** (Tocris #5387, Lille, France) or their vehicle (0.02% DMSO) was added to the media, according to the protocol described in Supporting Information Figure S1. The doses of thrombin used were selected according to previously published studies investigating the effects of thrombin in cell culture systems (Harmon *et al.*, 1986; Morganti *et al.*, 2010). Similarly, at the doses selected, the PAR1 (10 μM), and PAR4 (140 nM) antagonists were proven to specifically inhibit these receptors in cell culture models (Planty *et al.*, 2010; Young *et al.*, 2010; Wen *et al.*, 2014; Monjotin *et al.*, 2016). All cultures were stopped at day 6 for analysis.

Images of cultures and analysis

Structures were imaged using an apotome microscope (HXP120; Zeiss Axio-observer, Marly-le-roi France; 10 \times , 0.45 NA) from the Toulouse-Purpan Imaging Core facility directed by Sophie Allart. Images were analysed using the ImageJ software from Fiji. For immunostaining, organoids were analysed with an inverted confocal microscope, Spinning Disk (Flash4 CSU 1 \times , 234 z 0.5 μm , with stream, 20 \times 0.75 NA, 234 z-planes and 1.5 μm spacing). 3D reconstruction and analysis for each organoid acquired were done with Imaris software (8.2; Bitplane).

Classification of cultures

Structures were classified according to the presence of rounded or immature cells and budding between the harvesting and the 6 days of culture, as described by the intestinal stem cell consortium (Stelzner *et al.*, 2012) (a nomenclature for intestinal *in vitro* cultures). With regard to columnar structures, the cell polarity was defined by the polarized labelling of β -actin and β -catenin. A columnar cell was defined by a thickness >18 μm . Releasing structures were defined by a broken epithelium and the presence of cell debris inside and outside of the structure. For all structures, the diameters around the structure were measured four times, and measurements obtained were averaged. For budding structures, only the rounded core of the structure was measured for diameter; individual budding zones were not included in the diameter measurements.

Metabolic activity assay

The CellTiter-Glo[®] 3D reagent (Promega, #9683, Charbonniere-Les-Bains, France) kit was used to measure extracellular ATP, as an indication of mitochondrial metabolic activity within the cultures (Zanoni *et al.*, 2016). The reagent was added to the culture medium of each well (volume 1:1) and incubated for

30 min at RT, protected from light, as per the manufacturer's instructions. Luminescence was measured with a luminometer (Varioskan Flash – Thermo Scientific, Illkirch, France). A minimum of three wells per condition was analysed and measured and was calculated using an ATP standard curve. Because image acquisition of cells was not possible in the whole well, the ATP concentrations were normalized to the total surface area occupied by the cultured cell structures, as observed by microscopic analysis using bright field imaging using an apotome microscope. Therefore, the cell surface area was used to control for amount of tissue variation.

Apoptosis assay

Apoptosis was quantified using the NucView 488 caspase-3 kit (Ozyme, 1 mM in 1 \times PBS #BTM10403, Saint-Quentin-Fallavier, France), at day 6, where active caspase-3 is detected as a measure of apoptotic cells. As per the manufacturer's instructions, the NucView 488 reagent was added to culture medium of each well (volume 1:1) and incubated for 30 min at RT, and protected from light. Nuclei were stained using DAPI, as previously described (Gobbetti *et al.*, 2015). The fluorescence emitted was measured with a confocal microscope (Spinning Disk – CSU-X1 – Flash4 camera – 20 \times , 0.75 NA). Ten organoids were analysed per condition with 234 z-planes and 1.5 μm spacing, except for the second patient (thrombin 10 $\text{mU}\cdot\text{mL}^{-1}$ and F16357 10 μM , only two organoids were analysed) and the third patient (for the thrombin 50 $\text{mU}\cdot\text{mL}^{-1}$ condition, no organoid was analysed). The 3D reconstruction and analysis of number of caspase-3-positive cells (stained by DAPI as previously described; Cenac *et al.*, 2010) in the total number of cells in each organoid were done with Imaris software 8.2, Bitplane. Only caspase-3-positive cells present within the lining of the organoid epithelium were counted; positive cells present in the lumen were not considered.

Proliferation measurements

Organoids were fixed with 3.7% paraformaldehyde (PFA; Sigma-Aldrich, Saint-Quentin-Fallavier, France) in PBS at 37°C for 20 min. Organoids were permeabilized with 0.5% triton X-100 (Sigma-Aldrich, Saint-Quentin-Fallavier, France) in PBS at RT for 20 min and were incubated with a blocking buffer with 3% BSA (Sigma-Aldrich, Saint-Quentin-Fallavier, France) in PBS 1.5 h at 37°C. Organoids were then incubated for 2 h at 37°C with primary antibody anti-Ki67, mouse Ig G1 (Dako, #M7240, Les-Usis, France 1/100). Next, the primary antibody was washed out three times for 5 min, and organoids were incubated with the secondary antibody, AlexaFluor 568 donkey anti-mouse (Life Technologies, #A10038, Villebon-Sur-Yvette, France 1/500) for 1.5 h at 37°C and then stained for 20 min with DAPI (Invitrogen, Illkirch, France). Plates were mounted with Vectashield mounting medium (Eurobio, Les-Usis, France), and organoids were analysed with an inverted confocal microscope, Spinning Disk (Flash4 sCMOS, 234 z 0.5 μm , with stream, 20 \times 0.75 NA). All organoids were analysed for each condition with 234 z-planes and 1.5 μm spacing, more precisely as follows:

- First patient: control: 8 organoids analysed; thrombin 10 $\text{mU}\cdot\text{mL}^{-1}$: 7 organoids; thrombin 50 $\text{mU}\cdot\text{mL}^{-1}$: 6 organoids; thrombin 10 $\text{mU}\cdot\text{mL}^{-1}$ and ML354: 10 organoids; thrombin 50 $\text{mU}\cdot\text{mL}^{-1}$ and ML354: 10 organoids; thrombin

10 mU·mL⁻¹ and F16357: 10 organoids; thrombin 50 mU·mL⁻¹ and F16357: 10 organoids; ML354 140 nM: 7 organoids; and F16357 10 μM: 10 organoids.

- Second patient: control: 10 organoids analysed; thrombin 50 mU·mL⁻¹: 8 organoids; thrombin 10 mU·mL⁻¹ and ML354: 9 organoids; thrombin 50 mU·mL⁻¹ and ML354: 5 organoids; thrombin 10 mU·mL⁻¹ and F16357: 9 organoids; thrombin 50 mU·mL⁻¹ and F16357: 8 organoids; ML354 140 nM: 10 organoids; and F16357 10 μM: 5 organoids.
- Third patient: control: 10 organoids analysed; thrombin 10 mU·mL⁻¹: 8 organoids; thrombin 50 mU·mL⁻¹: 6 organoids; thrombin 10 mU·mL⁻¹ and ML354: 5 organoids; thrombin 50 mU·mL⁻¹ and ML354: 6 organoids; and thrombin 50 mU·mL⁻¹ and F16357: 5 organoids.
- Fourth patient: control: 7 organoids analysed; thrombin 10 mU·mL⁻¹: 10 organoids; thrombin 10 mU·mL⁻¹ and ML354: 5 organoids; thrombin 50 mU·mL⁻¹ and ML354: 6 organoids; thrombin 10 mU·mL⁻¹ and F16357: 10 organoids; thrombin 50 mU·mL⁻¹ and F16357: 6 organoids; ML354 140 nM: 10 organoids; and F16357 10 μM: 8 organoids.
- Fifth patient: control: 10 organoids analysed; thrombin 10 mU·mL⁻¹: 10 organoids; thrombin 50 mU·mL⁻¹: 7 organoids; thrombin 10 mU·mL⁻¹ and ML354: 7 organoids; thrombin 50 mU·mL⁻¹ and ML354: 6 organoids; thrombin 10 mU·mL⁻¹ and F16357: 5 organoids; thrombin 50 mU·mL⁻¹ and F16357: 6 organoids; ML354 140 nM: 7 organoids; and F16357 10 μM: 5 organoids.

3D reconstruction and analysis of Ki67-positive cells per total cells (stained by DAPI) in individual organoids were performed with Imaris software 8.2, Bitplane.

Real-time PCR

Total RNA was extracted from organoid cultures using TRIzol Plus RNA Purification Kit (Invitrogen, Illkirch, France) as previously described (D'Aldebert *et al.*, 2011). Real-time PCR was performed with PAR1 and PAR4 gene-specific primers: 5'AAGAAAGTCCGATCCCAGC3' and 5'TTTAACCTCC CAGCAGTCC3' for PAR1; 5'TGCGTGGATCCCTTCATCT AC3' and 5'CCTGCCCGCACCTTGTC3' for PAR4. The relative expression of targeted genes was compared with that of hypoxanthine phosphoribosyltransferase.

PAR1 immunohistochemistry

As for Ki67 immunostaining, organoids were fixed with 3.7% PFA (Sigma-Aldrich, Saint-Quentin-Fallavier, France) in PBS at 37°C for 20 min, permeabilized with 0.5% triton X-100 (Sigma-Aldrich, Saint-Quentin-Fallavier, France) in PBS at RT for 20 min and were incubated with a blocking buffer at 3% BSA (Sigma-Aldrich, Saint-Quentin-Fallavier, France) in PBS for 1.5 h at 37°C. Organoids were then incubated overnight with anti-PAR1 primary antibody (AB111976; Abcam, Cambridge, UK) at a concentration of 1:500 as previously described (Desormeaux *et al.*, 2018). After being washed, organoids were incubated with secondary antibody (Alexa Fluor) for 1 h, washed and mounted with Prolong Gold Reagent containing DAPI (Molecular Probes, Leiden, Netherlands), for nucleus staining. Controls for the specificity of the antibody include incubation in the absence of secondary antibody and in the presence of immunizing peptides (not shown).

Randomization, blinding and statistical analysis

All organoids present in wells were counted. For all experiments, plates were prepared so that all conditions were randomly present in each plate. Organoid counts and measures were performed by an observer unaware of the treatments.

Data are expressed as mean ± SEM. Analyses were performed using the GraphPad Prism 6.0 software. Statistical significance was determined by one-way ANOVA followed by Bonferroni multiple comparisons test. Significance was accepted for $P < 0.05$. *Post hoc* tests were run only if F achieved $P < 0.05$ and when no significant variance inhomogeneity was observed. The data and statistical analysis comply with the recommendations on experimental design and analysis in pharmacology (Curtis *et al.*, 2018).

Nomenclature of targets and ligands

Key protein targets and ligands in this article are hyperlinked to corresponding entries in <http://www.guidetopharmacology.org>, the common portal for data from the IUPHAR/BPS Guide to PHARMACOLOGY (Harding *et al.*, 2018), and are permanently archived in the Concise Guide to PHARMACOLOGY 2017/18 (Alexander *et al.*, 2017a,b).

Results

Characterization of organoid cultures

Human colon crypts were purified from fresh tissue samples obtained from colectomies harvested in healthy zones of tissues from patients diagnosed with colorectal cancer (Supporting Information Table S1). Isolated crypt fragments (Figure 1A, day 0 panel) were cultured in 3D Matrigel matrix for 3 and 6 days. Within the first day, the crypt architecture disappeared (not shown) to form organoid structures composed of an epithelial cell monolayer and a central lumen. At day 3 of culture, three types of structures were observed: 'cystic', 'columnar' and 'releasing' structures (Figure 1A, day 3 panel). Cystic structures were characterized by flat epithelial cells organized to delineate a clear lumen (Figure 1A). Epithelial cells comprising cystic organoids are typically immature and undifferentiated with high proliferative and self-renewal capacities (Ramalingam *et al.*, 2012; Stelzner *et al.*, 2012). Columnar structures were characterized by thicker epithelial cells, still monolayered, but with a columnar shape for all epithelial cells, similar to the shape of cells found in the native crypts (Figure 1A). Nuclei in columnar cells were stained on the basal portion of the cells. Epithelial cells from columnar structures typically undergo both proliferation and limited differentiation (Ramalingam *et al.*, 2012). The lumen of these structures could appear clear, or contain cellular debris. Releasing structures were characterized by their large size, the columnarity of the cells composing their shape and the presence of a crater that seems to allow the release of intraluminal debris (Figure 1A). At day 6 of culture, the same three types of structure were observed (Figure 1A, day 6 panel), and in addition, 'budding' structures were present. Budding structures are characterized by excrescences of new crypts and exemplify fully mature and differentiated organoids with both proliferative and differentiation capacities. These types of structures are called colonoids and were rare in our culture conditions (6 days of culture).

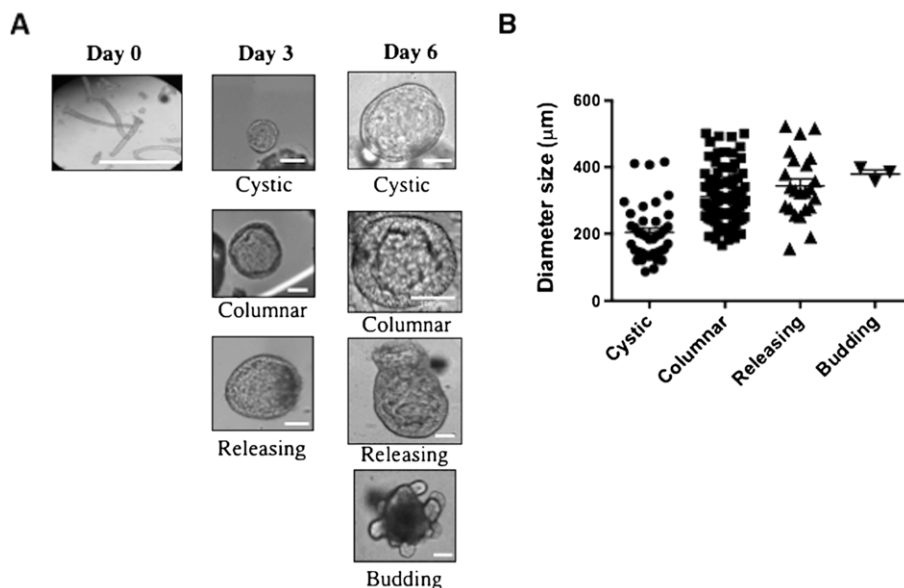


Figure 1

Organoid characterization. (A) Microphotographs of isolated crypts at day 0 of culture, representative cystic, columnar and releasing organoids at days 3 and 6 of culture and representative budding structure at day 6 of organoid culture. Scale bar is 100 μm . (B) Organoid diameter (μm), at day 6 of culture. Data are means \pm SEM, organoids $n = 39$ for cystic, $n = 85$ for columnar, $n = 23$ for releasing and $n = 3$ for budding. These data are representative of organoid cultures originating from five individuals.

The size of each type of structure was measured at day 6 of culture (Figure 1B) and showed a trend of increasing size from the most immature structures (cystic) to the most mature structures (releasing and budding).

Effects of thrombin exposure on human colon organoid cultures

Thrombin was added to the human organoid cultures daily from day 3 to day 6 of the culture (Supporting Information Figure S1). For the two doses of thrombin used (10 and 50 $\text{mU}\cdot\text{mL}^{-1}$), no difference in the total number of organoids was observed (not shown). Similarly, the size of cystic, columnar or releasing organoids was not changed by the addition of thrombin (Figure 2A). However, at the dose of 10 $\text{mU}\cdot\text{mL}^{-1}$, the addition of thrombin to human colon organoid cultures caused a significant decrease in the size of budding organoids, while the higher dose of 50 $\text{mU}\cdot\text{mL}^{-1}$ had no effect (Figure 2A).

While chronic incubation of human colon organoid cultures with thrombin had no effect on the percentage of columnar organoids present in the culture, thrombin (both 10 and 50 $\text{mU}\cdot\text{mL}^{-1}$) significantly affected the number of cystic organoids and increased the proportion of releasing organoids (Figure 2B). No significant effect was observed on the proportion of budding organoids in the presence of thrombin, but a trend towards an increased number of budding structures in the presence of thrombin could be noticed (Figure 2B). Taken together, these data suggest that thrombin exposure pushes colon organoid cultures towards maturation.

The concentration of ATP release per surface of total organoids was used as a measure of metabolic activity/cell survival in organoid cultures. Thrombin incubation (both at 10 and 50 $\text{mU}\cdot\text{mL}^{-1}$) significantly reduced the metabolic

activity of human colon organoid cultures (Figure 3). Apoptosis was significantly increased in epithelial cells lining within organoids exposed to both doses of thrombin (Figure 4). Immunostaining for apoptotic cells was particularly strong in the lumen of the structures (microphotographs on the panel) both in control conditions and after thrombin exposure. Such staining corresponds to physiological anoikis. However, in the case of thrombin exposure, apoptotic cells were also present within the cell lining of organoid structures (right panel photomicrograph). The percentage of proliferative cells (Ki67-positive cells) was significantly diminished in the presence of thrombin (both doses) (Figure 5).

Thrombin-induced effects on human colon organoid cultures are mediated by the activation of both PAR1 and PAR4

First, we investigated the presence of PAR1 and PAR4 in the material used. Both PAR1 and PAR4 mRNAs were detected in crypts isolated from human intestinal tissues (not shown). RT-PCR experiments showed that PAR1 and PAR4 mRNAs were present in 6 day organoid cultures, and this expression was significantly increased by exposure of cultures to increasing doses of thrombin (Figure 6A). Immunohistochemistry performed on organoids after 6 days of culture revealed that PAR1 was expressed on almost all epithelial cells (Figure 6B). Compared with the localization of the nucleus stained by DAPI, PAR1 expression appeared mostly on the basolateral side (Figure 6B). The addition of PAR1 or PAR4 antagonists alone to the cultures had no effect on the size of organoid subtypes (Supporting Information Figure S2), or on the types (cystic, columnar, releasing or budding) of organoids present

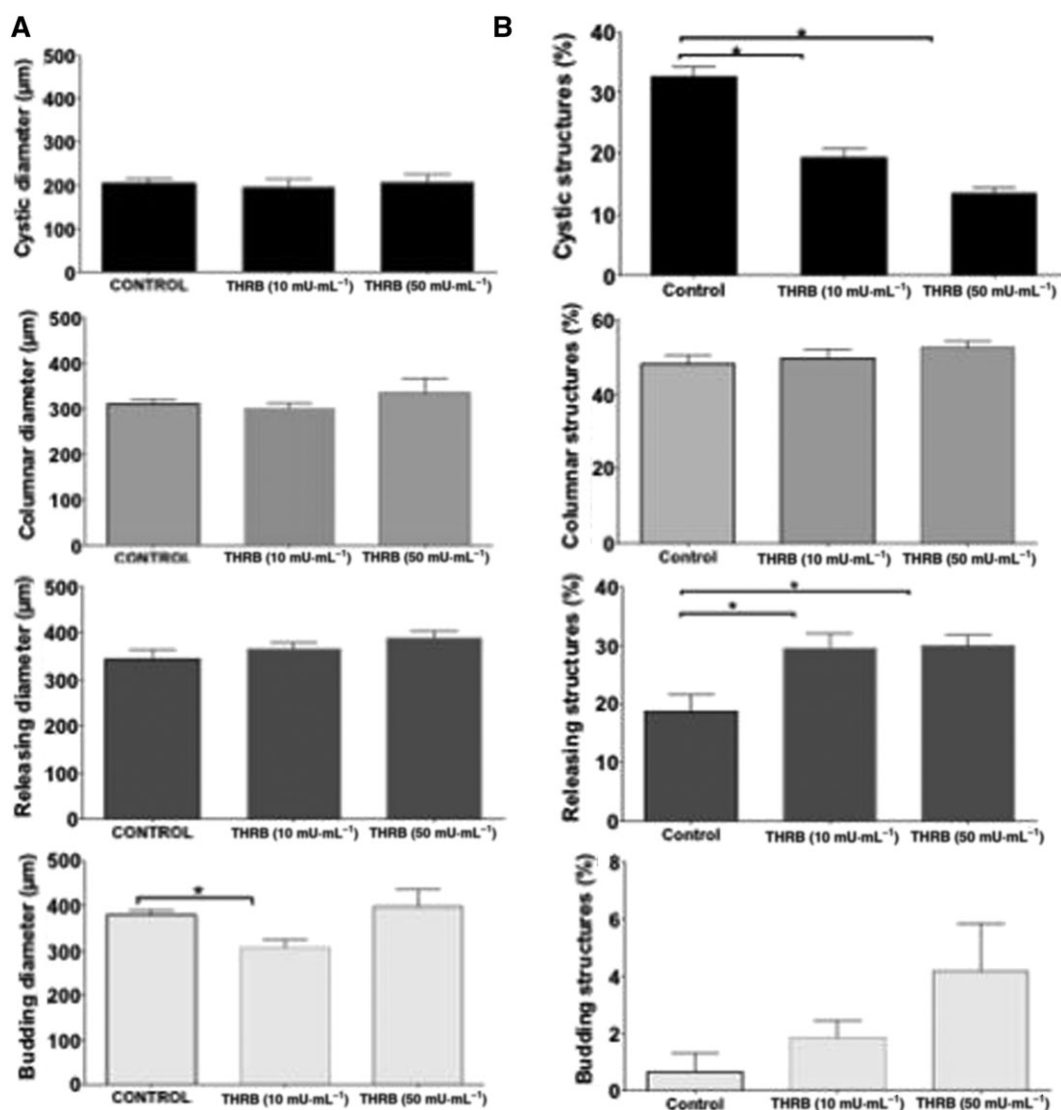


Figure 2

Effects of thrombin (THR) on organoid characteristics. (A) Diameter (μm) of cystic, columnar, releasing and budding organoids at 6 days of culture and after 3 days of exposure to thrombin at 10 or 50 $\text{mU}\cdot\text{mL}^{-1}$ or to vehicle. (B) The percentage of the different types of structures, at 6 days of culture and after 3 days of exposure to thrombin at 10 or 50 $\text{mU}\cdot\text{mL}^{-1}$ or to vehicle. Data are means \pm SEM with $n = 5$ different individuals from which tissues were harvested, and 70 organoids were analysed per condition. * $P < 0.05$ (one-way ANOVA, Bonferroni multiple comparisons test).

in the culture (Supporting Information Figure S2). Thrombin-induced decrease in per cent of cystic structures was reversed similarly by PAR1 and PAR4 antagonist treatment, independently of the dose of thrombin used (Figure 7A for the dose of 50 $\text{mU}\cdot\text{mL}^{-1}$, not shown for the 10 $\text{mU}\cdot\text{mL}^{-1}$ thrombin dose). Thrombin-induced increase in per cent of releasing structures was significantly reversed by PAR1 but not by PAR4 antagonist treatment, independently of the dose of thrombin used (Figure 7B for the dose of 50 $\text{mU}\cdot\text{mL}^{-1}$, not shown for the 10 $\text{mU}\cdot\text{mL}^{-1}$ dose). PAR4 antagonist treatment significantly decreased the per cent of budding structures observed in the presence of thrombin at the dose of 50 $\text{mU}\cdot\text{mL}^{-1}$ (Figure 7C). Thrombin had no effect on the per cent of columnar structures (Figure 2B), and treatments with PAR1 or PAR4 antagonist did not change this observation (data not shown). PAR1 or PAR4 antagonists had no effect on the size of

organoids exposed to thrombin, regardless of the dose of thrombin used (Supporting Information Figure S3). The decreased metabolic activity induced by the lowest dose of thrombin was inhibited by a pre-incubation with the PAR4 antagonist ML354 but not by the PAR1 antagonist F16357. In contrast, the effect of the highest dose of thrombin (50 $\text{mU}\cdot\text{mL}^{-1}$) was only inhibited by the PAR1 antagonist and not by the PAR4 antagonist (Figure 7D). The effects of all doses of thrombin on apoptosis were completely abolished by both the PAR1 and the PAR4 antagonists, indicating that both receptors play a role in thrombin-induced apoptosis, regardless of the dose (Figure 7E). Thrombin-induced decrease in percentage of proliferative cells was inhibited by the PAR4 antagonist for the low dose of thrombin (10 $\text{mU}\cdot\text{mL}^{-1}$) but not by the PAR1 antagonist (Figure 7F). The effects of the highest dose of thrombin (50 $\text{mU}\cdot\text{mL}^{-1}$) on

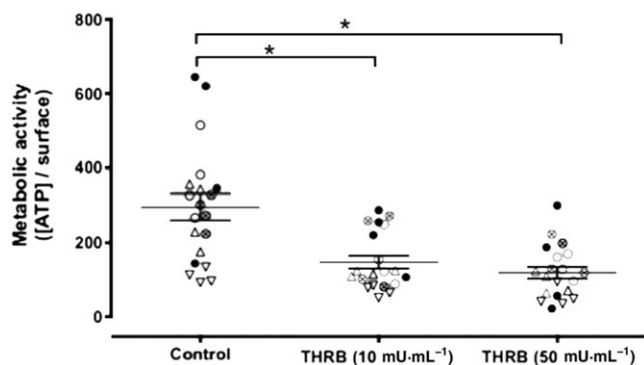


Figure 3

Effects of thrombin (THR B) on organoid metabolic activity. Concentration of ATP released per total surface of organoids as a measure of metabolic activity/cell survival in 6 day organoid cultures exposed to thrombin (10 or 50 mU·mL⁻¹) or to vehicle. Data are means ± SEM with $n = 5$ different individuals from which tissues were harvested. Individual sign shape represents data generated from the culture of the same patient tissue. * $P < 0.05$ (one-way ANOVA, Bonferroni multiple comparisons test).

the percentage of proliferative cells in organoid cultures were inhibited by the PAR1 but not by the PAR4 antagonist (Figure 7F).

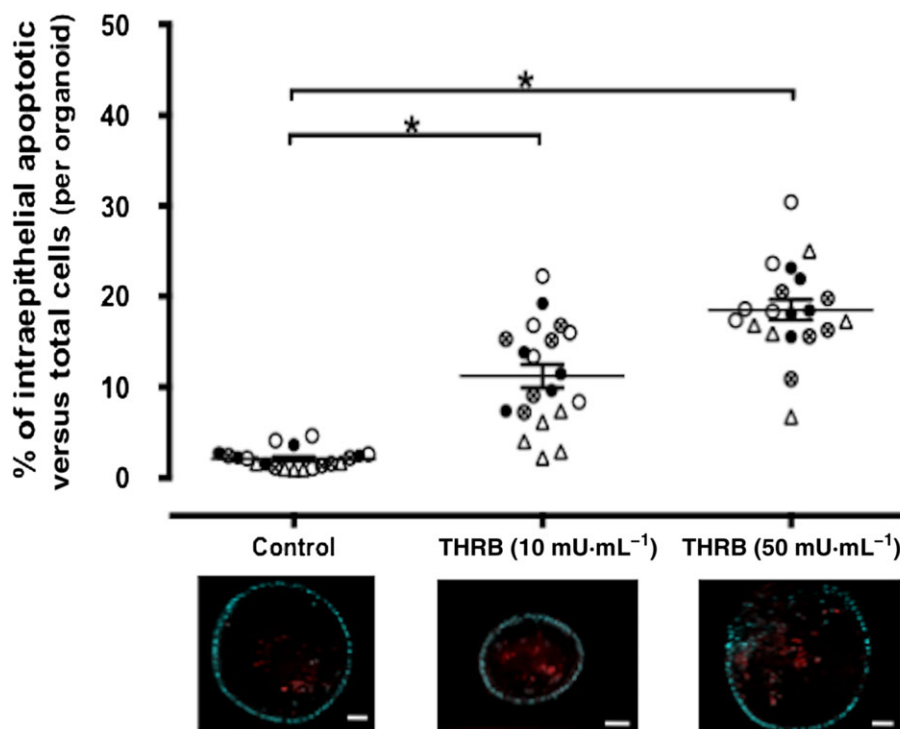


Figure 4

Effects of thrombin (THR B) on organoid cell apoptosis. The % of apoptotic cells (red staining) present in epithelial lining of organoid structures over total cells (cyan DAPI nucleus staining) per organoid cultured for 6 days and exposed for the last 3 days of culture to thrombin (10 or 50 mU·mL⁻¹) or vehicle. Data are means ± SEM with $n = 5$ different individuals from which tissues were harvested. Individual sign shape represents data generated from the culture of the same patient tissue. * $P < 0.05$ (one-way ANOVA, Bonferroni multiple comparisons test). Photomicrographs are representative pictures of caspase-3 staining in control condition (vehicle exposure) (left panel), thrombin 10 mU·mL⁻¹ incubation (middle panel) or thrombin 50 mU·mL⁻¹ (right panel) incubation. Scale bar is 50 μm.

Discussion

The present study investigated the effects of thrombin on the biology of the human intestinal epithelium, with the aim of determining whether exogenous thrombin could eventually modify epithelial growth and/or renewal. We demonstrated that exogenous thrombin favoured organoid maturation, also induced severe apoptosis, and reduced the metabolic activity and proliferation of human intestinal epithelial cells. Overall, our data suggest that the presence of thrombin in the vicinity of epithelial cells is detrimental to epithelial renewal. Furthermore, we demonstrated that these detrimental effects of thrombin are mediated by the activation of both PAR1 and PAR4, the two functional thrombin receptors. We have previously demonstrated that PAR1 is expressed in human and mouse colon crypts and organoids (Nasri *et al.*, 2016). The presence of PAR4 in stem cells/progenitors has not been previously demonstrated, but our results revealed an active role for PAR4 in these cells. These findings are particularly relevant in the context of IBD, where large amounts of thrombin are present in a patient's intestinal tissues (de Jong *et al.*, 1989). Potentially, thrombin could be present both on the basolateral side of epithelial cells as per blood vessel rupture and in the lumen upon bloody diarrhoea associated with IBD. Our data point to a basolateral effect of thrombin and its two receptors PAR1 and PAR4, as potential molecular targets for epithelial repair therapies. Indeed, previous studies have demonstrated a role

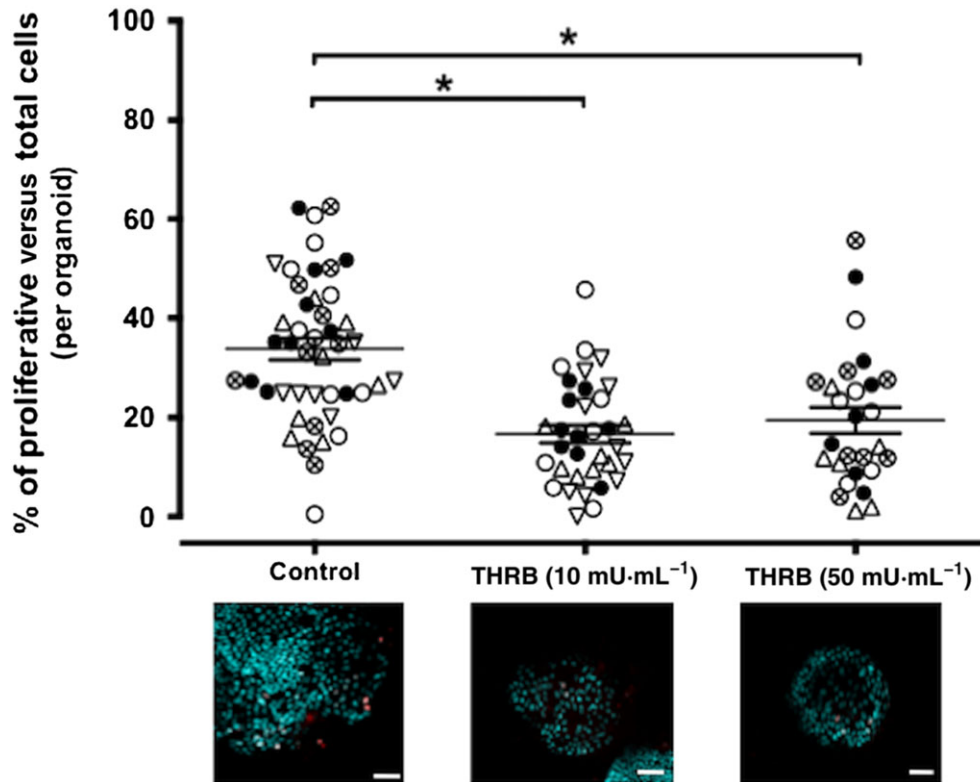


Figure 5

Effects of thrombin (THR) on organoid cell proliferation. The % of proliferative cells (Ki67 red staining) over total cells (cyan DAPI nucleus staining) per organoid cultured for 6 days and exposed for the last 3 days of culture to thrombin (10 or 50 $\text{mU}\cdot\text{mL}^{-1}$) or vehicle. Data are means \pm SEM with $n = 5$ different individuals from which tissues were harvested. Individual sign shape represents data generated from the culture of the same patient tissue. $*P < 0.05$ (one-way ANOVA, Bonferroni multiple comparisons test). Photomicrographs are representative pictures of Ki67 staining in control condition (vehicle exposure) (left panel), thrombin $10 \text{ mU}\cdot\text{mL}^{-1}$ incubation (middle panel) or thrombin $50 \text{ mU}\cdot\text{mL}^{-1}$ incubation. Scale bar is $50 \mu\text{m}$.

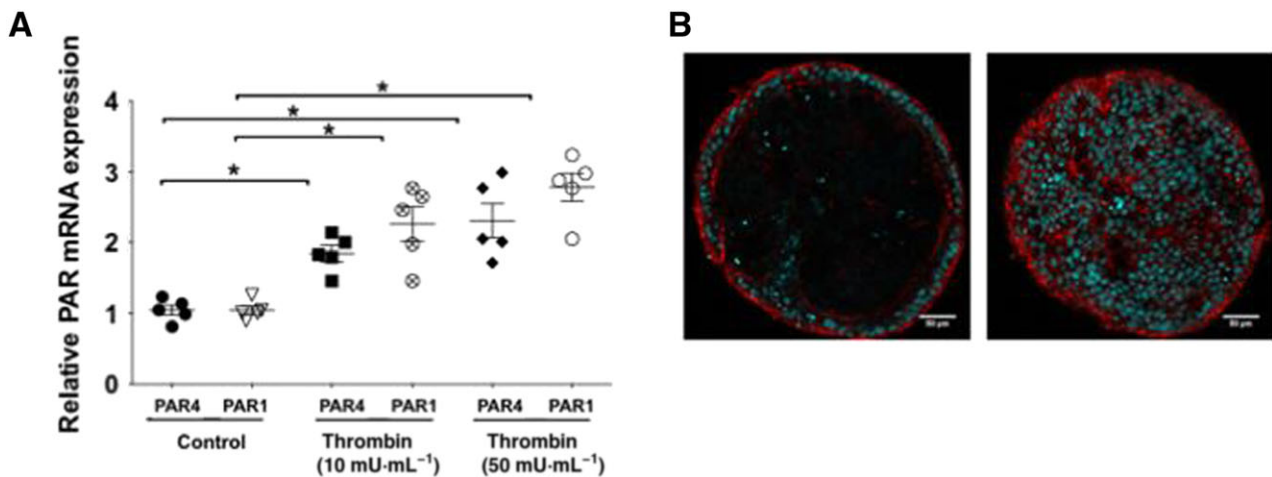


Figure 6

PAR1 and PAR4 expression in human colon organoid cultures. (A) Relative mRNA expression of PAR1 and PAR4 in 6 day organoid cultures exposed to vehicle (control) or to thrombin (10 and 50 $\text{mU}\cdot\text{mL}^{-1}$). (B) Photomicrographs representative of PAR1 immunostaining (red staining) and nucleus staining (blue staining with DAPI) in 6 day cultures of human colon organoids (two different z stack). Data in (A) are means \pm SEM of $n = 5$ different individuals from which tissues were harvested. $*P < 0.05$ (one-way ANOVA, Bonferroni multiple comparisons test). Scale bar is $50 \mu\text{m}$ in (B).

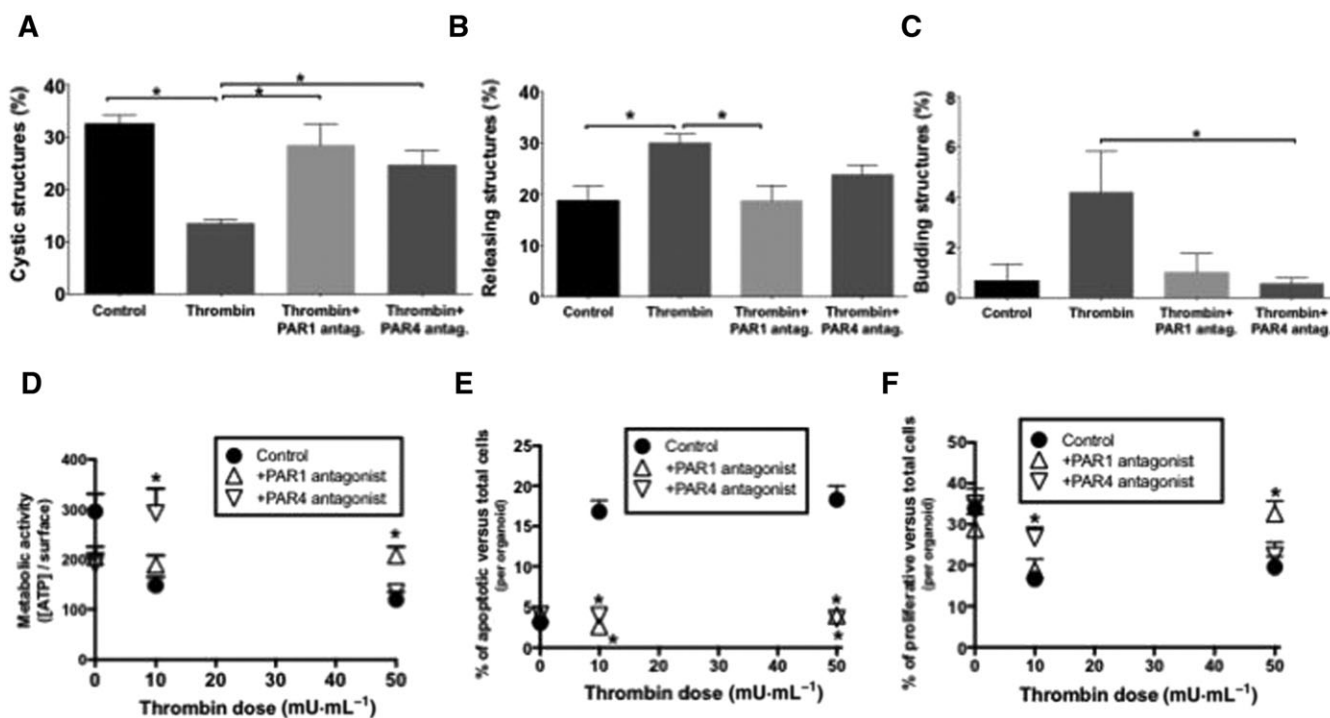


Figure 7

Effects of PAR1 and PAR4 antagonists on thrombin-induced changes in organoid composition, metabolic activity, apoptosis and cell proliferation. The % of (A) cystic organoids, (B) releasing organoids and (C) budding organoids, (D) ATP concentration, (E) % of apoptotic cells per organoid and (F) % of proliferative cells per organoid in response to thrombin (50 mU·mL⁻¹ for A–C and 10 or 50 mU·mL⁻¹ for D–F) added on the last 3 days of culture in the presence of PAR1 antagonist F16357 (10 μM), PAR4 antagonist ML354 (140 nM) or vehicle, in human organoid cultures for 6 days. Data are means ± SEM of *n* = 5 different individuals from which tissues were harvested. (F) The ratio of proliferative cells to total cells per organoid was calculated by use of Ki67 as a marker. **P* < 0.05 (one-way ANOVA, Bonferroni multiple comparisons test).

for PARs and PAR1 in particular in inflammation and in models of IBD (Vergnolle, 2004; Cenac *et al.*, 2005; Vergnolle, 2005; Vergnolle, 2009; Vergnolle, 2016).

Most importantly, the model we used is a model originating from the human colon and, replicating at its best, a human intestinal epithelial organ. This technology is based on the isolation of fresh intestinal crypts, which are then cultured in three dimensions. The intestinal stem cells present in the isolated crypts proliferate and enter into a differentiation process, recreating a complex epithelium, containing possibly all the cell types that compose the colonic epithelium (enteroendocrine cells, goblet cells, enterocytes, etc.) (Sato *et al.*, 2011). This model is nowadays considered as the best model to assess the effects of pharmacological treatments on human intestinal epithelium growth and regeneration (Cruz-Acuna *et al.*, 2017). Indeed, cultured organoids are proposed for regenerative therapies as their transplantation can contribute to tissue repair and regeneration after injury (Fordham *et al.*, 2013). Above all, this model offers an unparalleled strategy for recapitulating important features of human epithelial tissues and for testing pharmacological approaches.

Thrombin is massively present in the vicinity of intestinal epithelium in patients suffering from IBD. Indeed, bleeding is often associated with tissue injury, and bloody diarrhoea is a common symptom in IBD patients. In addition, studies have reported that IBD patients exhibit a threefold higher risk for

development of systemic thrombosis than the general population. An increased number of platelet aggregates and enhanced thrombin generation have been measured in IBD patients (Senchenkova *et al.*, 2015). The concentration of thrombin in tissues and blood from IBD patients is in the same range of concentrations we used in the present study, and the same concentrations of thrombin are classically used in *in vitro* models of platelet activation (de Jong *et al.*, 1989; Morganti *et al.*, 2010). Therefore, the effects of thrombin on human intestinal organoid cultures we observed could well be informative of the endogenous effects of thrombin in pathological situations such as IBD. In addition, by using the organoid model, we can speculate that the level of expression of thrombin receptors in intestinal epithelial cells is closer to physiological concentrations than those in cancer intestinal epithelial cell lines, which are known to overexpress PARs (Darmoul *et al.*, 2003; Gratio *et al.*, 2009). Therefore, thrombin's effects on human intestinal organoid cultures could be considered as representative of physiological or pathophysiological effects.

The incubation of organoid cultures in the presence of thrombin concomitantly reduced the percentage of cystic structures and increased the percentage of releasing structures. The squamous shape of cells in cystic structures is indicative of early immature structures, which have not yet acquired the columnar cell shape characteristic of mature colonic epithelium. Our data thus suggest that thrombin is able

to push organoid cultures towards a more mature phenotype. Although not significant, there was a trend towards an increased proportion of budding structures after thrombin exposure, in agreement with a pro-maturation effect of thrombin. The low number of budding structures at 6 days of culture might explain this lack of significance for thrombin's effects. These morphological evidences of a pro-maturation effect of thrombin should be completed by measuring differentiation markers. So far, we have investigated the mRNA expression of the two mucus proteins MUC2 and MUC5, but no effect of thrombin on their transcription could be detected in organoid cultures (not shown). In the future, more markers of all differentiated intestinal epithelial cells should be followed. Interestingly, concomitant to the pro-maturation effect, increased apoptosis was observed in organoid cultures in response to thrombin exposure. This was evidenced both by an increased staining for caspase-3 activity and by an increased number of releasing organoids: that is, structures full of apoptotic cells that are expelled from the organoid. Although thrombin could favour the acquisition of a more mature intestinal epithelium phenotype, overall thrombin did not favour organoid growth, as the size of cystic, columnar and releasing organoids was not modified by thrombin exposure. On the contrary, thrombin reduced the diameter of budding organoid structures. These structures are considered as the most mature organoid structures. Indeed, they present undifferentiated budding zones that correspond to the crypts and more differentiated zones at the top of those neo-formed crypts. The fact that thrombin exposure reduced the diameter of budding structures but not of cysts or columnar structures could suggest that thrombin inhibits the proliferation of a specific population of progenitors present in the developing buds. Indeed, we observed that thrombin exposure reduced the number of proliferative cells. Interestingly, at the lowest dose of thrombin used ($10 \text{ mU}\cdot\text{mL}^{-1}$, the same dose that lowered the diameter of budding structures), the anti-proliferative effect of thrombin was dependent on PAR4 activation. This could suggest that PAR4 activation slows organoid growth by inhibiting proliferation. However, at a higher dose of thrombin ($50 \text{ mU}\cdot\text{mL}^{-1}$), which had no effect on budding structure diameters, proliferation was still inhibited, but this time by a mechanism involving PAR1 activation and not PAR4 activation. This suggests that a compensatory mechanism might maintain the size of budding organoids in the presence of this high dose of thrombin, despite the anti-proliferative effects induced by PAR1 activation. In a previous study, we observed that PAR1-activating peptides increase the size of murine organoids in part by pushing differentiation processes (Nasri *et al.*, 2016). This could constitute the compensatory mechanism maintaining the size of budding organoids exposed to high doses of thrombin. Taken together, these data provide evidence that thrombin has an anti-proliferative effect that involves both PAR1 and PAR4 but differentially depending on the dose of thrombin.

The same differential involvement of PAR1 and PAR4 was observed for the effects of thrombin on metabolic activity measured in organoid cultures. At low doses of thrombin, PAR4 activation seemed to be involved, while at higher doses of thrombin, PAR1 activation seemed to be responsible for thrombin's effects. It is well known that not the same

concentrations of thrombin are required to activate PAR1 and PAR4 on platelets (Kahn *et al.*, 1998; Ramachandran and Hollenberg, 2008). However, in contrast to our findings, higher concentrations of thrombin are necessary to activate PAR4 because of the lack of a hirudin-like thrombin binding sequence on PAR4, while lower concentrations of thrombin are sufficient to activate PAR1, which possesses this binding sequence (Xu *et al.*, 1998). This apparent contradiction could be explained by the forms of thrombin that are present in the culture. While we added α -thrombin resuspended from lyophilized powder to the organoid cultures, this form of thrombin might not remain stable in organoid cultures, and depending on the presence of epithelial proteases, α -thrombin could be degraded to a certain extent to β -thrombin and/or γ -thrombin. α -Thrombin preferably binds and cleaves PAR1, but γ -thrombin is a much less potent agonist for PAR1 and more potent for PAR4 activation (Nystedt *et al.*, 1994; Xu *et al.*, 1998). Thus, depending on the concentration of thrombin we add and also depending on the presence of thrombin-cleaving proteases in our culture conditions, different forms of thrombin at different concentrations could be present and activate differentially PAR1 and PAR4. Indeed, in previous studies, we demonstrated that human intestinal epithelium is a major source of proteases (Motta *et al.*, 2011; Motta *et al.*, 2012; Rolland-Fourcade *et al.*, 2017), and these proteases, if released by organoid cultures, could cleave thrombin. Another potential explanation could be the occurrence of crosstalks with other members of the PAR family. For instance, PAR3 has been shown to act as a co-factor for PAR4 activation (Nakanishi-Matsui *et al.*, 2000). Depending on the expression of PAR3 together or not with PAR4 at the cell surface or intestinal epithelial cells, PAR1 or PAR4 activation might be favoured. Although PAR2 is not considered as a thrombin receptor, recent work from the Hollenberg's laboratory has demonstrated that thrombin can signal through PAR2 (Mihara *et al.*, 2016). We have previously shown that activated PAR2 strongly reduced the proliferation of immature cells, although without inducing apoptosis or decreasing stem cell capacities in mouse cultured organoids (Nasri *et al.*, 2016). Thus, PAR2 could be another player, activated at high concentrations of thrombin (Mihara *et al.*, 2016), interfering with proliferation and metabolic activity. Further experiments with selective peptidic agonists for the different PARs would bring important pharmacological information on the effects of each PARs. However, even the use of peptidic agonists is a limiting factor as tethered ligand peptides do not reproduce all signalling pathways triggered by PAR-activating proteases (Ramachandran and Hollenberg, 2008).

Interestingly, both the PAR1 or PAR4 antagonist alone (in the absence of thrombin) decreased metabolic activity by one-third in organoid cultures (Figure 7D, time 0). One can speculate that some proteases are present in intestinal epithelial cells and could constitutively activate PAR1 and PAR4 in steady states, lowering metabolic activity. Trypsin-3, a protease known to activate PAR1 and PAR4 (Knecht *et al.*, 2007), has recently been shown to be present in intestinal epithelial cells (Rolland-Fourcade *et al.*, 2017); this protease could be responsible for this effect.

It is important to note, however, that the cell assay that was used in the present study to measure ATP levels is also reported as an indicator of cell viability. In order to fully discuss

the effects of thrombin on metabolic activity, other parameters such as glycolysis, oxygen consumption or NADH activity should be measured.

The most striking effect of thrombin on human colon organoid cultures was on the induction of apoptosis. Apoptosis is a physiological process in intestinal epithelium, where highly differentiated cells at the top of the crypt undergo apoptosis in order to be renewed. However, excess of apoptosis could be harmful to the mucosa, leading to an increased permeability and an increased presence of immature cells (Blander, 2016). It has been shown that IBD is associated with increased epithelial cell apoptosis and increased permeability, the aberrant epithelial cell death being responsible at least in part, for the delayed mucosal healing (Blander, 2016). Considering the high amounts of thrombin present in tissues from IBD patients, and the pro-apoptotic effects we observed for thrombin in human intestinal organoid cultures, it is plausible to think that in IBD patients, the presence of thrombin in the vicinity of the epithelium participates to the increased apoptosis. Indeed, here by counting only apoptotic cells present within the epithelium lining of organoids, our results point to direct pro-apoptotic effect of thrombin on functional epithelial cells and not only an increased anoikis. This clearly suggests a detrimental effect for thrombin on functional epithelium. Further, we demonstrated that both PAR1 and PAR4 activations are involved in the mechanism of thrombin-induced apoptosis in intestinal epithelial cells. In previous studies, we have demonstrated that PAR1 activation provoked an increased permeability due to aberrant apoptosis. This was demonstrated both *in vitro* in epithelial cancer cell line cultures and *in vivo* in a mouse model (Chin *et al.*, 2003). The results from the present study definitively point to the possible same mechanism in non-transformed complex human epithelium and add to the mechanism the possible involvement of PAR4.

Conclusions

The present study demonstrated the multiple effects of thrombin in human intestinal epithelium, identifying PAR1 and PAR4 as important receptors mediating these effects. While the pharmacological approach used here suggests that the regulation of PAR1 and PAR4 activation by thrombin could be subtle in human intestinal epithelial cells, depending on the concentration of surrounding thrombin, all our data point to a detrimental effect of thrombin and its receptors on epithelial growth and potential healing. These findings seem particularly relevant in the context of IBD, where thrombin is largely present in the vicinity of epithelial cells, and suggest that thrombin inhibition, PAR1 and PAR4 blockade could constitute a possible therapeutic intervention in IBD to favour epithelial regrowth and barrier function. However, it is important to note that our study was performed in healthy tissues, and different responses to thrombin could be expected in tissues from IBD patients. Furthermore, by favouring differentiation and maturation, thrombin through the activation of PAR1 and PAR4 could also exert positive effects on epithelial repair. Further studies are necessary to investigate the effects of thrombin and PAR activation in

organoid cultures from IBD patients, discriminating between Crohn's disease and ulcerative colitis.

Acknowledgements

The authors thank Astrid Canivet and Sophie Allart from the Imaging Core Facility of Toulouse-Purpan for their help with 3D imaging and analysis. This work was supported by a grant from the European Research Council (ERC-310973 PIPE) to N.V. Tissue collection was originally sponsored by the University Hospital of Toulouse for regulatory and ethic submission and by a grant from the delegation régionale à la recherche clinique des hôpitaux de Toulouse, through the MICILIP project. The COLIC collection (DC-2015-2443) was used in the present study. This project was also supported through a 'Fond Unique Interministeriel' (FUI) programme, by the Région Midi-Pyrénées (now Occitanie), Toulouse Métropole, the Banque Publique d'Investissement (BPI) de France. Equipments obtained from the use of Fonds Européens de Développement Régional (FEDER) and the region Occitanie were used in the present research programme.

Author contributions

M.S. performed the experiments, analysed the data and contributed to the draft manuscript. L.A., G.P., N.M. and D.B. provided material and helped to edit the manuscript. A.D.-S., S.C., P.L., C.R.-S., D.B., A.F. and N.V. analysed and critically reviewed the data, obtained funding and contributed to the editing of the manuscript. A.D.-S., A.F. and N.V. designed, conceived and supervised the study. N.V. wrote the manuscript, and editing was performed by all the authors.

Conflict of interest

The authors declare no conflicts of interest.

Declaration of transparency and scientific rigour

This Declaration acknowledges that this paper adheres to the principles for transparent reporting and scientific rigour of preclinical research recommended by funding agencies, publishers and other organisations engaged with supporting research.

References

Alexander SPH, Christopoulos A, Davenport AP, Kelly E, Marrion NV, Peters JA *et al.* (2017a). The Concise Guide to PHARMACOLOGY 2017/18: G protein-coupled receptors. *Br J Pharmacol* 174 (Suppl 1): S17–S129.

- Alexander SPH, Fabbro D, Kelly E, Marrion NV, Peters JA, Faccenda E *et al.* (2017b). The Concise Guide to PHARMACOLOGY 2017/18: enzymes. *Br J Pharmacol* 174 (Suppl 1): S272–S359.
- Blander JM (2016). Death in the intestinal epithelium – basic biology and implications for inflammatory bowel disease. *FEBS J* 283: 2720–2730.
- Cenac N, Altier C, Motta JP, d'Aldebert E, Galeano S, Zamponi GW *et al.* (2010). Potentiation of TRPV4 signalling by histamine and serotonin: an important mechanism for visceral hypersensitivity. *Gut* 59: 481–488.
- Cenac N, Cellars L, Steinhoff M, Andrade-Gordon P, Hollenberg MD, Wallace JL *et al.* (2005). Proteinase-activated receptor-1 is an anti-inflammatory signal for colitis mediated by a type 2 immune response. *Inflamm Bowel Dis* 11: 792–798.
- Chin AC, Vergnolle N, MacNaughton WK, Wallace JL, Hollenberg MD, Buret AG (2003). Proteinase-activated receptor 1 activation induces epithelial apoptosis and increases intestinal permeability. *Proc Natl Acad Sci U S A* 100: 11104–11109.
- Crespo M, Vilar E, Tsai SY, Chang K, Amin S, Srinivasan *Tet al.* (2017). Colonic organoids derived from human induced pluripotent stem cells for modeling colorectal cancer and drug testing. *Nat Med* 23: 878–884.
- Cruz-Acuna R, Quiros M, Farkas AE, Dedhia PH, Huang S, Siuda D *et al.* (2017). Synthetic hydrogels for human intestinal organoid generation and colonic wound repair. *Nat Cell Biol* 19: 1326–1335.
- Curtis MJ, Alexander S, Cirino G, Docherty JR, George CH, Gienbycz MA *et al.* (2018). Experimental design and analysis and their reporting II: updated and simplified guidance for authors and peer reviewers. *Br J Pharmacol* 175: 987–993.
- D'Aldebert E, Cenac N, Rousset P, Martin L, Rolland C, Chapman K *et al.* (2011). Transient receptor potential vanilloid 4 activated inflammatory signals by intestinal epithelial cells and colitis in mice. *Gastroenterology* 140: 275–285.
- Darmoul D, Gratio V, Devaud H, Lehy T, Laburthe M (2003). Aberrant expression and activation of the thrombin receptor protease-activated receptor-1 induces cell proliferation and motility in human colon cancer cells. *Am J Pathol* 162: 1503–1513.
- de Jong E, Porte RJ, Knot EA, Verheijen JH, Dees J (1989). Disturbed fibrinolysis in patients with inflammatory bowel disease. A study in blood plasma, colon mucosa, and faeces. *Gut* 30: 188–194.
- Desormeaux C, Bautzova T, Garcia-Caraballo S, Rolland C, Barbaro MR, Brierley SM *et al.* (2018). Protease-activated receptor 1 is implicated in irritable bowel syndrome mediators-induced signalling to thoracic human sensory neurons. *Pain* 159: 1257–1267.
- Fordham RP, Yui S, Hannan NR, Soendergaard C, Madgwick A, Schweiger PJ *et al.* (2013). Transplantation of expanded fetal intestinal progenitors contributes to colon regeneration after injury. *Cell Stem Cell* 13: 734–744.
- Gobbetti T, Ducheix S, le Faouder P, Perez T, Riols F, Boue J *et al.* (2015). Protective effects of *n*-6 fatty acids-enriched diet on intestinal ischaemia/reperfusion injury involve lipoxin A4 and its receptor. *Br J Pharmacol* 172: 910–923.
- Gratio V, Walker F, Lehy T, Laburthe M, Darmoul D (2009). Aberrant expression of proteinase-activated receptor 4 promotes colon cancer cell proliferation through a persistent signaling that involves Src and ErbB-2 kinase. *Int J Cancer* 124: 1517–1525.
- Harding SD, Sharman JL, Faccenda E, Southan C, Pawson AJ, Ireland S *et al.* (2018). The IUPHAR/BPS guide to pharmacology in 2018: updates and expansion to encompass the new guide to immunopharmacology. *Nucl Acids Res* 46: D1091–D1106.
- Harmon JT, Tandon NN, Hoeg JM, Jamieson GA (1986). Thrombin binding and response in platelets from patients with dyslipoproteinemias: increased stimulus-response coupling in type II hyperlipoproteinemia. *Blood* 68: 498–505.
- Iacucci M, Ghosh S (2016). Mucosal healing – how deep is enough? *Dig Dis* 34: 160–164.
- Kahn ML, Zheng YW, Huang W, Bigornia V, Zeng D, Moff S *et al.* (1998). A dual thrombin receptor system for platelet activation. *Nature* 394: 690–694.
- Knecht W, Cottrell GS, Amadesi S, Mohlin J, Skaregarde A, Gedda K *et al.* (2007). Trypsin IV or mesotrypsin and p23 cleave protease-activated receptors 1 and 2 to induce inflammation and hyperalgesia. *J Biol Chem* 282: 26089–26100.
- Mihara K, Ramachandran R, Saifeddine M, Hansen KK, Renaux B, Polley D *et al.* (2016). Thrombin-mediated direct activation of proteinase-activated receptor-2: another target for thrombin signaling. *Mol Pharmacol* 89: 606–614.
- Monjotin N, Gillespie J, Farrie M, Le Grand B, Junquero D, Vergnolle N (2016). F16357, a novel protease-activated receptor 1 antagonist, improves urodynamic parameters in a rat model of interstitial cystitis. *Br J Pharmacol* 173: 2224–2236.
- Morganti RP, Cardoso MH, Pereira FG, Lorand-Metze I, De Nucci G, Marcondes S *et al.* (2010). Mechanisms underlying the inhibitory effects of lipopolysaccharide on human platelet adhesion. *Platelets* 21: 260–269.
- Motta JP, Bermudez-Humaran LG, Deraison C, Martin L, Rolland C, Rousset P *et al.* (2012). Food-grade bacteria expressing elafin protect against inflammation and restore colon homeostasis. *Sci Transl Med* 4: 158ra144.
- Motta JP, Magne L, Descamps D, Rolland C, Squarzone-Dale C, Rousset P *et al.* (2011). Modifying the protease, antiprotease pattern by elafin overexpression protects mice from colitis. *Gastroenterology* 140: 1272–1282.
- Nakanishi-Matsui M, Zheng YW, Sulciner DJ, Weiss EJ, Ludeman MJ, Coughlin SR (2000). PAR3 is a cofactor for PAR4 activation by thrombin. *Nature* 404: 609–613.
- Nasri I, Bonnet D, Zwarycz B, d'Aldebert E, Khou S, Mezghani-Jarraya R *et al.* (2016). PAR2-dependent activation of GSK3 β regulates the survival of colon stem/progenitor cells. *Am J Physiol Gastrointest Liver Physiol* 311: G221–G236.
- Nystedt S, Emilsson K, Wahlestedt C, Sundelin J (1994). Molecular cloning of a potential proteinase activated receptor. *Proc Natl Acad Sci U S A* 91: 9208–9212.
- Planty B, Pujol C, Lamothe M, Maraval C, Horn C, Le Grand B *et al.* (2010). Exploration of a new series of PAR1 antagonists. *Bioorg Med Chem Lett* 20: 1735–1739.
- Ramachandran R, Hollenberg MD (2008). Proteinases and signalling: pathophysiological and therapeutic implications via PARs and more. *Br J Pharmacol* 153 (Suppl. 1): S263–S282.
- Ramalingam S, Daughtridge GW, Johnston MJ, Gracz AD, Magness ST (2012). Distinct levels of Sox9 expression mark colon epithelial stem cells that form colonoids in culture. *Am J Physiol Gastrointest Liver Physiol* 302: G10–G20.

Rolland-Fourcade C, Denadai-Souza A, Cirillo C, Lopez C, Jaramillo JO, Desormeaux C *et al.* (2017). Epithelial expression and function of trypsin-3 in irritable bowel syndrome. *Gut* 66: 1767–1778.

Sato T, Stange DE, Ferrante M, Vries RG, Van Es JH, Van den Brink S *et al.* (2011). Long-term expansion of epithelial organoids from human colon, adenoma, adenocarcinoma, and Barrett's epithelium. *Gastroenterology* 141: 1762–1772.

Senchenkova E, Seifert H, Granger DN (2015). Hypercoagulability and platelet abnormalities in inflammatory bowel disease. *Semin Thromb Hemost* 41: 582–589.

Shah SC, Colombel JF, Sands BE, Narula N (2016). Mucosal healing is associated with improved long-term outcomes of patients with ulcerative colitis: a systematic review and meta-analysis. *Clin Gastroenterol Hepatol* 14: 1245, e1248–1255.

Stelzner M, Helmrath M, Dunn JC, Henning SJ, Houchen CW, Kuo C *et al.* (2012). A nomenclature for intestinal in vitro cultures. *Am J Physiol Gastrointest Liver Physiol* 302: G1359–G1363.

Vergnolle N (2004). Modulation of visceral pain and inflammation by protease-activated receptors. *Br J Pharmacol* 141: 1264–1274.

Vergnolle N (2005). Clinical relevance of proteinase activated receptors (pars) in the gut. *Gut* 54: 867–874.

Vergnolle N (2009). Protease-activated receptors as drug targets in inflammation and pain. *Pharmacol Ther* 123: 292–309.

Vergnolle N (2016). Protease inhibition as new therapeutic strategy for GI diseases. *Gut* 65: 1215–1224.

Wen W, Young SE, Duvernay MT, Schulte ML, Nance KD, Melancon BJ *et al.* (2014). Substituted indoles as selective protease activated receptor 4 (PAR-4) antagonists: discovery and SAR of ML354. *Bioorg Med Chem Lett* 24: 4708–4713.

Xu WF, Andersen H, Whitmore TE, Presnell SR, Yee DP, Ching A *et al.* (1998). Cloning and characterization of human protease-activated receptor 4. *Proc Natl Acad Sci U S A* 95: 6642–6646.

Young SE, Duvernay MT, Schulte ML, Nance KD, Melancon BJ, Engers J, *et al.* (2010). A novel and selective PAR4 antagonist: ML354. In *Probe Reports from the NIH Molecular Libraries Program*. Bethesda (MD).

Zanoni M, Piccinini F, Arienti C, Zamagni A, Santi S, Polico R *et al.* (2016). 3D tumor spheroid models for in vitro therapeutic screening: a systematic approach to enhance the biological relevance of data obtained. *Sci Rep* 6: 19103.

Supporting Information

Additional supporting information may be found online in the Supporting Information section at the end of the article.

<https://doi.org/10.1111/bph.14430>

Figure S1 Schedule of experiments. Kinetic scheme of organoid cultures, from crypt isolation (day 0), to the addition of thrombin (10 or 50 mU.mL⁻¹) or vehicle, in the presence or not of PAR1-, PAR4- antagonists or their vehicle (from day 3 to day 6). All analyses were performed at day 6.

Figure S2 Effects of PAR1 and PAR4 antagonists on organoid characteristics. A – Organoid diameter (μm) of cystic, columnar, releasing and budding organoids at 6-days of culture and after 3 days of exposure to PAR1 or PAR4 antagonist alone. B – Repartition of the different types of structures, at 6-days of culture and after 3 days of exposure to PAR1 or PAR4 antagonist alone. Data are means ±SEM with n=5 individuals from which tissues were harvested. One-way ANOVA was performed and F did not achieve P < 0.05.

Figure S3 Effects of PAR1 and PAR4 antagonists on the effects of Thrombin on organoid diameter. Organoid diameter (μm) of cystic, columnar, releasing and budding organoids at 6-days of culture and after 3 days of exposure to Thrombin 10 mU.ml⁻¹ (A), or Thrombin 50 mU.ml⁻¹ (B), and in the presence of vehicle, PAR1 or PAR4 antagonist. Data are means ±SEM with n = 5 individuals from which tissues were harvested. One-way ANOVA was performed and F did not achieve P < 0.05.

Table S1 Characteristics and outcomes of control patients (NS: not-specified; NSAIDs: non-steroidal anti-inflammatory drugs).